

Optimization of Naphthalimide-imidazoacridone with Potent Antitumor Activity Leading to Clinical Candidate (HKH40A, RTA 502)

Humcha K. Hariprakash,[†] Teresa Kosakowska-Cholody,[†] Colin Meyer,[§] Wieslaw M. Cholody,[†] Sherman F. Stinson,[‡] Nadya I. Tarasova,^{*,†} and Christopher J. Michejda^{†,||}

Molecular Aspects of Drug Design Section, Structural Biophysics Laboratory, Center for Cancer Research, NCI-Frederick, Frederick, Maryland 21702, Developmental Therapeutics Program, NCI-Frederick, Frederick Maryland 21702, and Reata Pharmaceuticals, 2801 Gateway Drive, Suite 150, Irving, Texas

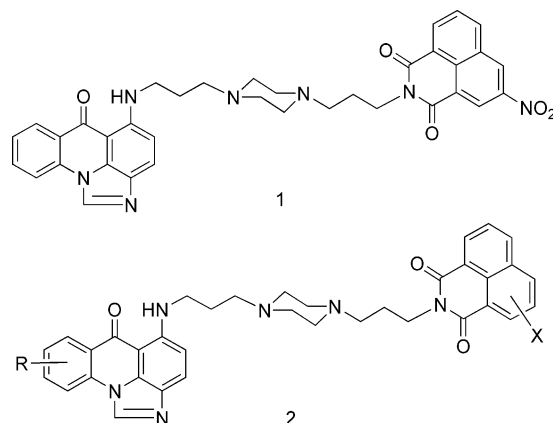
Received August 6, 2007

Abstract: Unsymmetrical bifunctional antitumor agent WMC79 was further optimized to generate compound **7b** that not only inhibited the growth of many tumor cell lines, but caused rapid apoptosis. Unlike the parent compound, **7b** is toxic to both p53 positive and negative cancer cells. It has potent in vivo activity against xenografts of human colon and pancreatic tumors in athymic mice.

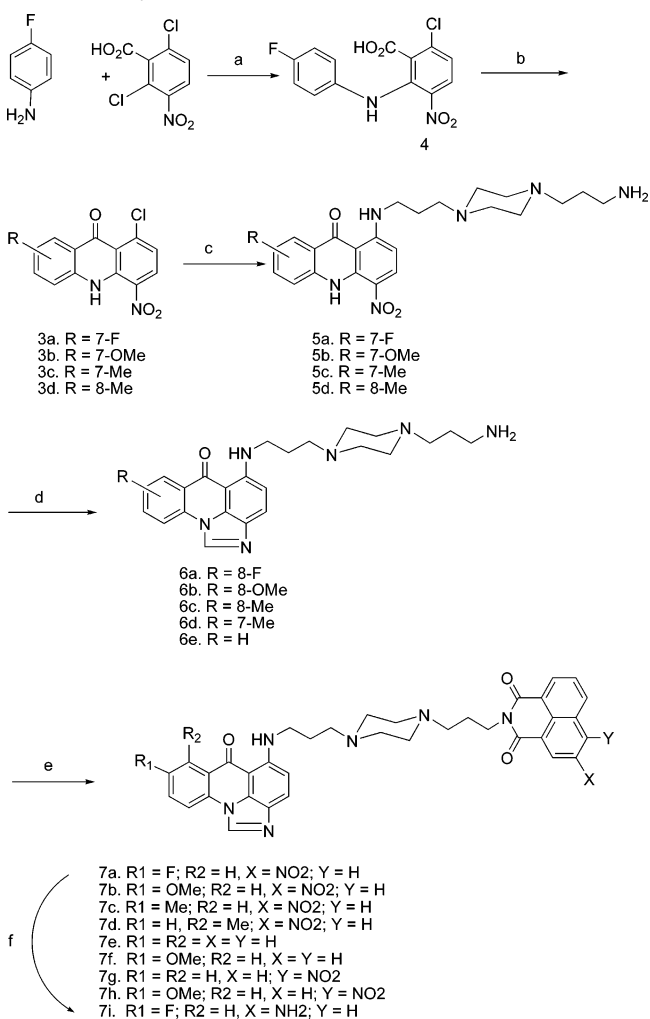
Many currently used anticancer drugs have multiple molecular targets.¹ Multitargeting may carry a significant advantage in cancer therapy because tumor growth is caused by multiple mutations.² Frequently, activation of more than one signaling pathway defines cancerous cell phenotype. DNA-binding compounds present a class of multipotent antitumor agents. Complexity and heterogeneity of DNA structure in the cells defines significantly different effects of different DNA-binding compounds on cellular events.

We have been working on a class of molecules that contain two different DNA-binding moieties linked together with a linker that can also facilitate binding to DNA.^{3–7} Even slight variations in the structure of these compounds tend to lead to significant changes in their biological properties. Here we report optimization of a previously reported compound **1** (WMC79; Chart 1)^{5,8} into a highly potent agent with remarkable and selective antitumor activity. Cell toxicity of **1** is p53-dependent and, thus, it has lower potency against p53-negative cells. The compound is also poorly soluble. We focused our structure optimization efforts on modifications in the positions 7 and 8 of the imidazoacridone ring as well as on substitutions in the 1,8-naphthalimide moiety. The general synthetic routes for the new compounds are presented in Scheme 1. The fluorinated acridone **3a** was obtained in an analogous manner from 4-fluoroaniline, as described previously for **3b–d**.⁹ Condensation of 2,6-dichloro-3-nitrobenzoic acid and 4-fluoroaniline led to the acid **4**, which upon acylation resulted in the fluorinated acridone **3a**. Heating the acridones **3** with excess of 1,4-bis(3-aminopropyl)piperazine, as described earlier,⁸ in either dimethylformamide (DMF^a) or dimethylsulfoxide (DMSO) gave the nitroacridones **5**, which were cyclized to the imidazoacridones **6a–d**. The unsubstituted compound **6e** has been reported recently.⁸ Imidazoacridones **6** were then condensed with equimolar

Chart 1. Structures of **1** and New Derivatives (**2**)



Scheme 1. Synthesis of Derivatives of **1**^a



^a Reagents and conditions: (a) EtOH, reflux; (b) POCl₃, CHCl₃, reflux; (c) 1,4-bis(3-aminopropyl)piperazine, DMF (for **5a**) or DMSO (for **5b–d**); (d) for **6a**, Ra–Ni/H₂, HCO₂H; then HCl, reflux; for **6b–d**, SnCl₂, HCO₂H, HCl, reflux; (e) naphthalic anhydride, DMF, 80 °C; (f) SnCl₂, HCO₂H, HCl, reflux.

lar amounts of appropriate naphthalic anhydrides, resulting in compounds **7a–h**. Compound **7a** was further transformed to the amino derivative **7i** by reduction of the nitro group with stannous chloride.

* To whom correspondence should be addressed. Tel.: 301-846-5225. Fax: 301-846-6231. E-mail: tarasova@ncifcrf.gov.

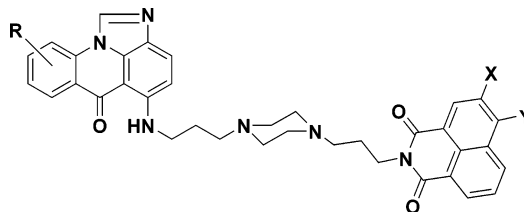
[†] Molecular Aspects of Drug Design Section, Structural Biophysics Laboratory, Center for Cancer Research, NCI-Frederick.

[‡] Developmental Therapeutics Program, NCI-Frederick.

[§] Reata Pharmaceuticals.

^{||} Passed away on January 9, 2007.

^a Abbreviations: DMF, *N,N*-dimethylformamide; DMSO, dimethyl sulfoxide; MTT, 3-(4,5-dimethylthiazol-2-yl)-2,5-diphenyltetrazolium bromide.

Table 1. In Vitro Activity of **1** and Derivatives **7** against Selected Human Cancer Cell Lines^a


cmpd	R	X	Y	tumor cell lines					
				HCT116		HT29		Hep3B	
				GI ₅₀ (nM)	LC ₅₀ (nM)	GI ₅₀ (nM)	LC ₅₀ (nM)	GI ₅₀ (nM)	LC ₅₀ (nM)
7a	8-F	NO ₂	H	1	40	2	600	4	400
7b	8-OMe	NO ₂	H	1	30	1	80	2.5	50
7c	8-Me	NO ₂	H	3.5	30		NT ^b		NT ^b
7d	7-Me	NO ₂	H	3	30		NT ^b		NT ^b
7e	H	H	H	15	1000	11	1000	22	1000
7f	8-OMe	H	H	3.5	70	3	1000	3.5	330
7g	H	H	NO ₂	5.5	>1000	15	1000	18	1000
7h	8-OMe	H	NO ₂	3	350	4	1000	5	800
7i	8-F	NH ₂	H	2.2	80	8	750		NT ^b
1	H	NO ₂	H	1	40	2	550	4	380

^a Measured by a 5 day MTT assay. The obtained data was used to calculate GI₅₀, TGI, and LC₅₀ values presented. Values shown are means ± SD of at least three independent experiments. The coefficients of variation were between 10 and 20%. ^b NT, not tested.

For biological testing, all new compounds (**7**) were transformed into their tri(methanesulfonate) salts, that were sufficiently soluble in water and in dilute buffers. All of the compounds reported are very stable in the solid state, especially in the methanesulfonate form, but suffer photochemical degradation when dilute solutions are exposed to ambient light for prolonged periods of time. The compounds are easily adsorbed on glass and quartz surfaces, which affect the concentrations of dilute solutions significantly. These solutions were not affected by polyethylene or polycarbonate surfaces.

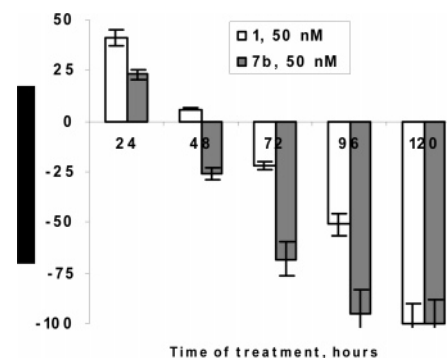
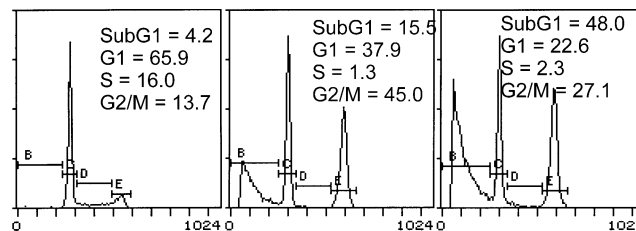
All new derivatives had comparable growth inhibitory activities in p53-positive HCT116 colon tumor cell line (Table 1). However, the activity in the ability to kill cancer cells differed significantly. The nitro group in position 5 of the naphthalimide ring was essential for the cell-killing activity of the compounds. Eliminating it (as in **7f**) resulted in about a 10-fold reduction in LC₅₀. Reduction of the nitro group into an amino group (**7i**) caused a slight increase in LC₅₀. Compounds with a nitro group in position 6 rather than 5 (**7g** and **7h**) had significantly lower cell-killing activity. Position 8 of the imidazoacridone ring is known to undergo metabolic hydroxylation that may have a negative effect on the in vivo activity of the compounds. In an attempt to improve the metabolic stability of the compounds, we have evaluated derivatives with a fluorine atom in position 8 (**7a** and **7i**). The compounds were equal in activity to the unsubstituted parent compound, **1**; however, they turned out to be much less soluble. Similarly, methyl derivatives (**7c** and **7d**) had significantly reduced solubility. On the contrary, methoxy derivatives were more soluble than unsubstituted counterparts and had much improved antitumor activity.

The unsubstituted naphthalimide ring gave rise to the least active of the compounds (**7e**; Table 1). A comparison of antitumor potency of **1** and **7b** in the NCI 60 human tumor cell line screen, which is based on a short 48 h continuous drug exposure, showed about 30-fold higher cell killing activity of **7b** (median LC₅₀ = 0.67 μM compared to 19.9 μM for **1**). Because killing of tumor cells by a drug can be a slow process

Table 2. In Vitro Activity of **1** and **7b** against Selected Human Tumor Cell Lines^a

cell line	LC ₅₀ (nM)	
	cmpd 1	cmpd 7b
HCT116 (wild-type p53)	40	30
RKO (wild-type p53)	40	25
Colo205 (mutated p53)	500	80
HT29 (mutated p53)	550	80
ASPC-1 (p53 null)	350	70
10.05 (mutated p53)	300	90
PC3 (mutated p53)	>1000	45

^a Determined by a 5 day MTT assay.

**Figure 1.** Time-dependent cytotoxicity of **1** and **7b**, measured by MTT assay in HCT116 colon cancer cells.**Figure 2.** Effects of **1** and **7b** on cell-cycle distribution in HCT116 cells exposed to compounds for 72 h.

frequently requiring much more than 48 h, we evaluated the cytotoxic effects in a 5 day assay. Table 2 presents results from this experiment for selected cell lines that differ in the status of p53. The growth inhibition effect (GI₅₀) of both compounds was very similar (1–5 nM) for all tested cell lines regardless of the status of p53. In contrast, there was a significant difference between the two compounds in their cell killing ability. For **1**, the LC₅₀ is clearly about 10-fold higher for cell lines with mutated or null p53, while the LC₅₀ values for **7b** were superior in all tested cell lines.

Time course analysis of HCT116 cells exposed to **1** and **7b** performed at different concentrations indicated that **7b** needed much shorter incubation time to exhibit cytotoxic activity (Figure 1). Treatment of HCT116 cells with **7b** at 50 nM caused visible cell killing already after 48 h, whereas **1** required much longer exposure to achieve similar effect. The cell-killing effects were confirmed by cell cycle analysis (Figure 2). A 72 h treatment of HCT116 cells with 50 nM of either drug resulted in the appearance of sub-G₁ population corresponding to dead cells that represented 15.5% and 48.0%, respectively, for **1** and **7b**. At the same time, there was a significant accumulation of cells in the G₂/M phase (45.0% and 27.1% compared to 13% in control cells), decrease in the G₁ phase (from 65.9% in untreated cells to 37.9% and 22.6%, respectively), and almost total depletion of cells in the S-phase.

Pilot pharmacokinetic studies conducted in CD2F1 mice after i.v. injection of **1** or **7b** showed that the total plasma clearance

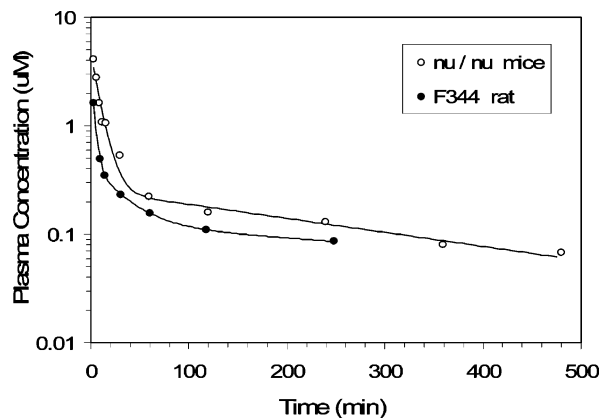


Figure 3. Blood plasma concentrations of **7b** following i.v. administration at a dose of 20 mg/kg body to ncr nu/nu mice and to a F344 rat. Lines represent the respective lines of best fit determined by nonlinear regression analysis.

rate of **7b** was 35% lower than that of **1** (238 vs 323 mL/min/kg, respectively). Because of the more favorable pharmacokinetic and biological features of **7b** compared to **1**, more comprehensive evaluations of **7b** were performed. In both nu/nu mice and F344 rats, disposition of **7b** following i.v. injection at a dose of 20 mg/kg was typified by a rapid initial “distribution” phase (6 and 2 min, respectively) and a long terminal “elimination” phase (4 and 8 h, respectively, Figure 3).

The terminal disposition phases accounted for a high proportion (70% in mice, and 82% in rats) of the total areas under the plasma concentration versus time curves. Initial (3 min) plasma concentrations were 4.1 μM and 1.6 μM in mice and rats, respectively. Plasma levels of **7b** were 70 nM after 8 h in mice and 90 nM after 4 h in rats. In both species, the apparent volumes of distribution of **7b** were very high relative to its apparent volumes of the central (plasma) compartments (57 vs 5 L/kg, respectively, in mice and 138 vs 6 L/kg, respectively, in rats), suggesting that **7b** is highly distributed into the tissues in these species.

In both mice and rats, **7b** was not detected in the plasma (l.o.d = 50 nM) when it was given by the i.p. or p.o. routes, strongly suggesting that **7b** is rapidly metabolized and eliminated by the liver after being absorbed into the hepatic portal circulation. Also, **7b** was not detected in plasma samples when it was administered s.c. to nude mice, demonstrating that i.v. injection offers the most promising route of administration for in vivo efficacy studies with **7b**. When given i.v. in a single well-tolerated dose, plasma levels of **7b** exceeded concentrations required for in vitro efficacy for up to 8 h in mice and 4 h in rats.

Compound **7b** dose-dependently inhibited growth of HCT116 xenografts in vivo, with a maximum TGI of 59% (Figure 4). This compound significantly inhibited growth of PaCa-2 pancreatic xenografts, which has mutated p53, in vivo with maximum growth inhibition of 53.5% at 15 mg/kg and significantly outperformed gemcitabine, a standard agent for the treatment of pancreatic tumors (TGI = 85.3%). The combination of **7b** and gemcitabine performed better than both single agents and induced regression over days 11 through 18 (Figure 5). No toxicity was detected for **7b** at the doses tested.

In conclusion, structure optimization of **1** revealed that introduction of the methoxy group in position 8 of the imidazoacridone ring improved in vitro and in vivo potency of the parent compound. Based on its enhanced overall profile, compound **7b** (HKH40a, RTA502) was chosen for IND filing and further clinical development.

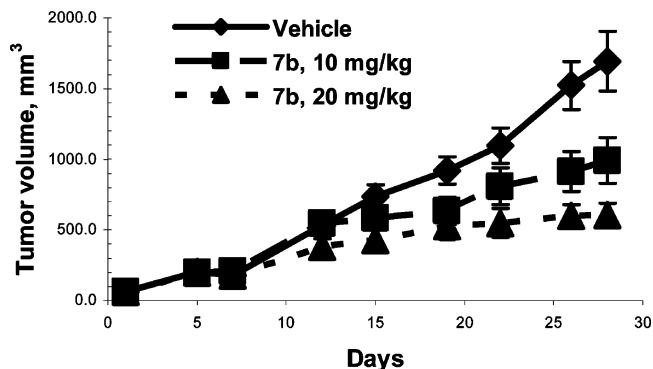


Figure 4. Inhibition of colon tumor growth in mice. HCT-116 colon cancer tumor fragments were implanted on the flank of nu/nu mice, seven animals in each group. Treatment (iv administration, Q3Dx4) was started when tumors reached 62 mm³.

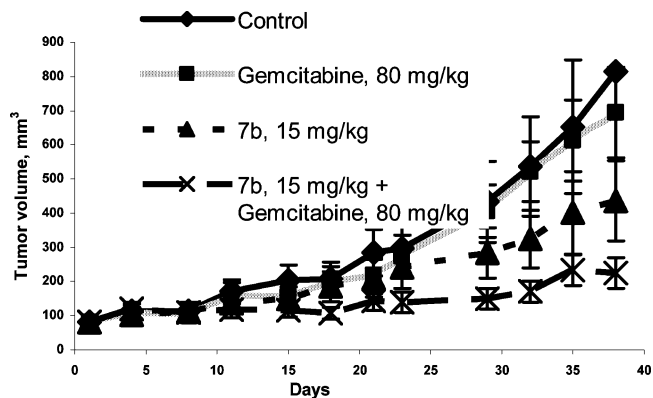


Figure 5. Inhibition of pancreatic tumor growth in mice in comparison and in combination with gemcitabine. PaCa-2 tumor fragments were implanted on the flank of nu/nu mice (10 in each group). Treatment (intraperitoneal, Q3Dx4) started 12 days post-inoculation when tumors reached 80 mm³.

Acknowledgment. We are very grateful to Dr. Larry Keefer for the critical reading of the manuscript, to Dr. Dominic Scudiero for the NCI 60 cell line assay data, and to Dr. Sergey Tarasov for discussions. We thank the Structural Biophysics Resource, SBL, NCI-Frederick, for the use of the mass spectrometer. This research was supported in part by the Intramural Research Program, the National Institutes of Health, National Cancer Institute, Center for Cancer Research.

Supporting Information Available: Experimental details and analytical data for the compounds described and NCI 60 cell lines screening data for **7b**. This material is available free of charge via the Internet at <http://pubs.acs.org>.

References

- (1) Kamb, A.; Wee, S.; Lengauer, C. Why is cancer drug discovery so difficult? *Nat. Rev. Drug Discovery* **2007**, *6*, 115–120.
- (2) Sjoblom, T.; Jones, S.; Wood, L. D.; Parsons, D. W.; Lin, J.; Barber, T. D.; Mandelker, D.; Leary, R. J.; Ptak, J.; Silliman, N.; Szabo, S.; Buckhaults, P.; Farrell, C.; Meeh, P.; Markowitz, S. D.; Willis, J.; Dawson, D.; Willson, J. K.; Gazdar, A. F.; Hartigan, J.; Wu, L.; Liu, C.; Parmigiani, G.; Park, B. H.; Bachman, K. E.; Papadopoulos, N.; Vogelstein, B.; Kinzler, K. W.; Velculescu, V. E. The consensus coding sequences of human breast and colorectal cancers. *Science* **2006**, *314*, 268–274.
- (3) Cholody, W. M.; Hernandez, L.; Hassner, L.; Scudiero, D. A.; Djurickovic, D. B.; Michejda, C. J. Bisimidazoacridones and related compounds: New antineoplastic agents with high selectivity against colon tumors. *J. Med. Chem* **1995**, *38*, 3043–3052.
- (4) Cholody, W. M.; Kosakowska-Cholody, T.; Michejda, C. J. Bisimidazoacridones induce a potent cytostatic effect in colon tumor cells that sensitizes them to killing by UCN-01. *Cancer Chemother. Pharmacol.* **2001**, *47*, 241–249.

- (5) Kosakowska-Cholody, T.; Cholody, W. M.; Monks, A.; Woy-narowska, B. A.; Michejda, C. J. WMC-79, a potent agent against colon cancers, induces apoptosis through a p53-dependent pathway. *Mol. Cancer Ther.* **2005**, *4*, 1617–1627.
- (6) Tarasov, S. G.; Casas-Finet, J. R.; Cholody, W. M.; Michejda, C. J. Bisimidazoacridones: Effect of molecular environment on conformation and photophysical properties. *Photochem. Photobiol.* **1999**, *70*, 568–578.
- (7) Tarasov, S. G.; Casas-Finet, J. R.; Cholody, W. M.; Kosakowska-Cholody, T.; Gryczynski, Z. K.; Michejda, C. J. Bisimidazoacridones: 2. Steady-state and time-resolved fluorescence studies of their diverse interactions with DNA. *Photochem. Photobiol.* **2003**, *78*, 313–322.
- (8) Cholody, W. M.; Kosakowska-Cholody, T.; Hollingshead, M. G.; Hariprakash, H. K.; Michejda, C. J. A new synthetic agent with potent but selective cytotoxic activity against cancer. *J. Med. Chem.* **2005**, *48*, 4474–4481.
- (9) Lehmstedt, K.; Schrader, K. Synthesis in the acridone series. *Chem. Ber.* **1937**, *70*, 1526.

JM7009777